Hindawi Publishing Corporation
Advances in Materials Science and Engineering
Volume 2015, Article ID 586264, 19 pages
http://dx.doi.org/10.1155/2015/586264

Research Article

Locally Corroded Stiffener Effect on Shear Buckling Behaviors of Web Panel in the Plate Girder

Jungwon Huh,[1] In-Tae Kim,[2] and Jin-Hee Ahn[3]

[1]*Department of Ocean Civil Engineering, Chonnam National University, Yeosu, Jeonnam 550-749, Republic of Korea*
[2]*Department of Civil Engineering, Pusan National University, Busan 609-735, Republic of Korea*
[3]*Department of Civil Engineering, Gyeongnam National University of Science and Technology, Jinju, Gyeongnam 660-758, Republic of Korea*

Correspondence should be addressed to Jin-Hee Ahn; jhahn@gntech.ac.kr

Received 15 April 2015; Revised 17 June 2015; Accepted 25 June 2015

Academic Editor: Antônio G. B. de Lima

The shear buckling failure and strength of a web panel stiffened by stiffeners with corrosion damage were examined according to the degree of corrosion of the stiffeners, using the finite element analysis method. For this purpose, a plate girder with a four-panel web girder stiffened by vertical and longitudinal stiffeners was selected, and its deformable behaviors and the principal stress distribution of the web panel at the shear buckling strength of the web were compared after their post-shear buckling behaviors, as well as their out-of-plane displacement, to evaluate the effect of the stiffener in the web panel on the shear buckling failure. Their critical shear buckling load and shear buckling strength were also examined. The FE analyses showed that their typical shear buckling failures were affected by the structural relationship between the web panel and each stiffener in the plate girder, to resist shear buckling of the web panel. Their critical shear buckling loads decreased from 82% to 59%, and their shear buckling strength decreased from 88% to 76%, due to the effect of corrosion of the stiffeners on their shear buckling behavior. Thus, especially in cases with over 40% corrosion damage of the vertical stiffener, they can have lower shear buckling strength than their design level.

1. Introduction

In steel plate girder bridges with more than 50–70 years' service period, severe corrosion damaged structural members have been found near their supports from their corrosive environmental condition, such as higher humidity caused by poor air circulation, dust deposition, and rain water or antifreeze penetration from drainage type expansion joints [1–3]. For a steel plate girder bridge, vertical and longitudinal stiffeners are basically installed to improve the shear buckling strength of their web panel. However, stiffeners also are not free from corrosion damage, depending on time-dependent maintenance. In the collapsed plate girder bridge caused by severe corrosion damage in Japan in 2009 [3, 4], severely corroded longitudinal and vertical stiffeners were also found, as shown in Figure 1. For shear buckling problems, various studies were conducted to examine the shear bucking behaviors of web panel and to suggest design guideline of web panel under shear loading [5–12]. Several studies on shear buckling problem with local corrosion damage in web panel were also carried out, since corrosion damage of the web panel is related to decrease in the shear buckling strength and shear failure behavior [2, 3, 13–17]. In case of a corroded plate girder, sectional damage of stiffeners affected by corrosion damage can also relate to shear buckling behaviors of the web panel. However, it is difficult to consider all the corroded cases of a plate girder. If all cases were considered, the corrosion damage effect of a stiffener on the shear buckling behaviors of a plate girder is not clear.

In this study, therefore, a stiffener was only selected as a corroded member of a plate girder. Nonlinear FE analyses of web panels stiffened by stiffeners were conducted, to compare their shear buckling behaviors according to the degree of corrosion of their stiffeners. Thus, a plate girder with a four-panel web panel stiffened by vertical and longitudinal stiffeners was selected. After their post-shear buckling behaviors, their shear buckling failures were compared, as well as their change in shear buckling strength. Then, the effect of the corroded

(a) After collapse [3] (b) Inside before collapse [4]

Figure 1: A collapsed steel plate girder bridge in Japan [3, 4].

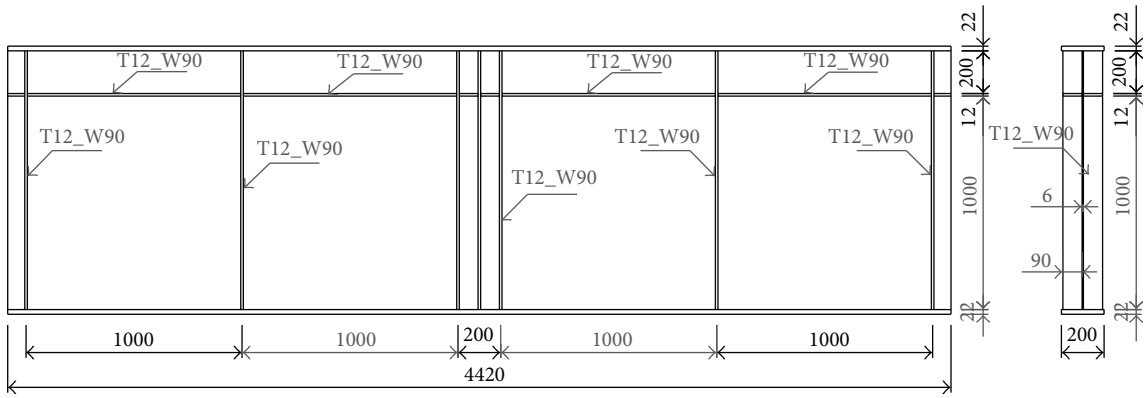

Figure 2: Dimensions of web panel and stiffener for FE analysis.

stiffener of the web panel on the shear buckling failure was evaluated.

2. FE Analysis Model of Plate Girder with Corroded Stiffener

2.1. Analysis Cases of the Corroded Stiffener in the FE Analysis. To numerically analyze the shear buckling behaviors of the web panel with stiffener, a four-panel web plate girder stiffened by vertical stiffeners and longitudinal stiffeners was selected, with a total height of 1,256 mm (stiffened web panel, with height and width of 1000 mm), a total length of 4,420 mm, flange width of 200 mm, flange thickness of 22 mm, and web thickness of 6 mm, as shown in Figure 2. All the stiffeners were considered identical, of 12 mm thickness and 90 mm width.

In this study, the FE analysis models were classified into three cases, depending on the analysis conditions. For the first FE analysis case, a plate girder with longitudinal stiffener was selected to examine the shear buckling behaviors affected by the vertical stiffener; thus only the vertical stiffener was considered to be corroded from the lower flange in the plate girder. For the second FE analysis case, the vertical stiffener and end-longitudinal stiffener were considered to be corroded from the lower flange and center of the end-longitudinal stiffener, to examine the effect between the corroded vertical stiffener and the end-longitudinal stiffener on their shear buckling behaviors. For the third FE analysis case, a left-longitudinal stiffener (end-longitudinal stiffener) and right-longitudinal stiffener (next-longitudinal stiffener) were considered to be corroded with the vertical stiffener, to examine the relationship between left-longitudinal stiffener and right-longitudinal stiffener. Thus, in the vertical and left-longitudinal stiffener corrosion model, the corroded height of the vertical stiffener changed from 0 mm to 1000 mm in 100 mm units (10% of the vertical stiffener height), and the corroded width of the left-longitudinal stiffener changed from 0 mm to 1000 mm from the center of longitudinal stiffener in 200 mm units (20% of vertical stiffener height) for a symmetric web panel, as shown in Figure 3(a). In the vertical and left-right longitudinal stiffener corrosion model, the corroded height of the vertical stiffener changed from 0 mm to 500 mm in 100 mm units (10% of the vertical stiffener height), and the corroded width of the left-longitudinal stiffener changed from 200 mm to 800 mm in 200 mm units (20% of vertical stiffener height), and the right-longitudinal stiffener changed to 400 mm and 800 mm for a symmetric web panel, as shown in Figure 3(b). However, the corroded widths of the left-longitudinal stiffener and right-longitudinal stiffener were not the same for all analysis cases, to examine the relationship between the end-longitudinal stiffener and the next-longitudinal stiffener.

For the FE analysis model, they are identified as follows: the first letter indicates the analysis case (VL: vertical and left-longitudinal stiffener corrosion model, V-L-R: vertical and left-right longitudinal stiffener corrosion model), the second letter, H, indicates the corrosion height of the vertical stiffener (e.g., H200 indicates a corroded vertical stiffener of 200 mm from the lower flange), the third letter, L, indicates the width of the left-longitudinal stiffener (e.g., L200 indicates an

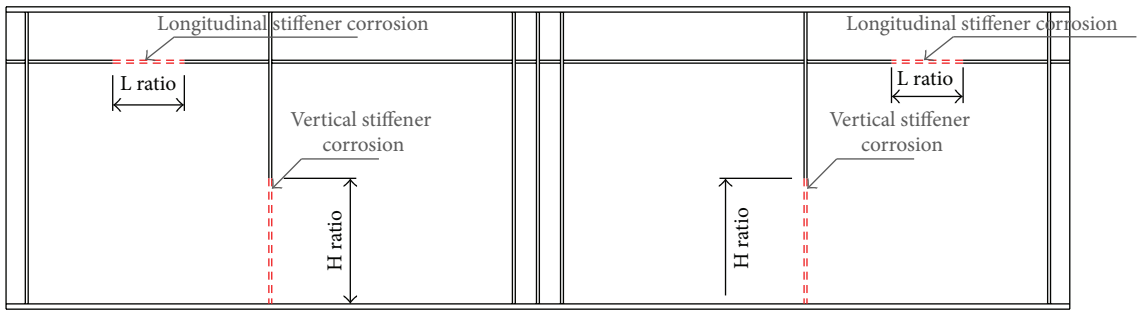

(a) Vertical and end-longitudinal stiffener corrosion model (V-stiffener cases, V-L stiffener cases)

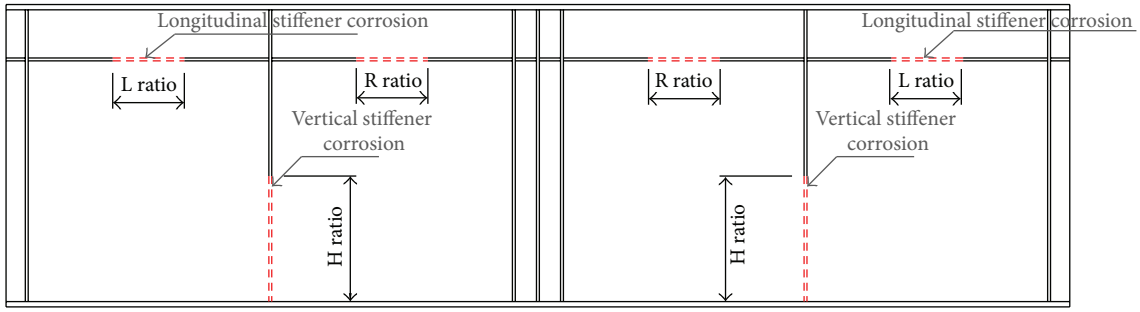

(b) Vertical and left-right longitudinal stiffener corrosion model (V-L-R stiffener cases)

Figure 3: Corrosion damage condition of web stiffener for FE analysis.

end-longitudinal stiffener of 200 mm), and the fourth letter, R, indicates the width of the right-longitudinal stiffener (e.g., R200 indicates the next-longitudinal stiffener of 200 mm).

Therefore, in this study, the corrosion ratio of vertical and longitudinal stiffeners for each FE analysis can be summarized as follows:

(1) Vertical stiffener corrosion model (V-stiffener cases).

(2) Vertical and left-longitudinal stiffener corrosion model (V-L stiffener cases).

(3) Vertical and left-right longitudinal stiffener corrosion model (V-L-R stiffener cases).

2.2. FE Analysis Model. In order to examine the shear buckling failure of the web panel related to the locally corroded stiffener condition in the plate girder using nonlinear FE analysis (finite element analysis), the FE analysis program MARC Mentat 2010 was used for each of the stiffener corrosion cases. To determine their critical shear buckling loads, buckling modes, elastic buckling analysis was anteriorly conducted before postbuckling analysis. Then, their incremental nonlinear analyses with elastic buckling modes were sequentially processed. In this FE analysis model, an 8-node solid element was used, as shown in Figure 4. For material properties of the FE analysis model, the tensile strength test results were used with a nominal yield stress of 260 MPa, Young's modulus of 206,000 MPa, and Poisson's ratio of 0.3. Elastic-perfectly plastic behaviors and the von Mises yield criterion were applied as the material plasticity.

For boundary conditions of the FE analysis model, both the lower flanges of the end panel (Boundary A) only were released to rotate in the transverse direction, while the other translations and rotations were prevented. For its symmetrical behavior, five points of the upper flange (Boundary B) in the plate girder model were not allowed to translate in the transverse direction, and a center point (Boundary C) at the lower flange was not allowed to translate in the longitudinal direction. For the shear bucking of the web panel, shear load was applied to the center flange of the FE analysis model. Each FE analysis case was considered corrosion damage conditions of their vertical and longitudinal stiffeners. For vertical stiffener corrosion models, a lower part of vertical stiffener was removed as corrosion damage as 100 mm units from the lower flange in the plate girder. For longitudinal stiffener corrosion models with vertical stiffener corrosion, center part of end-longitudinal stiffener and right-longitudinal stiffener (next-longitudinal stiffener) was removed with the corrosion damage of vertical stiffeners according to FE analysis condition. For V-LH600L400 model, therefore, vertical stiffener was removed to 600 mm from lower flange and 400 mm length of end-longitudinal stiffener was removed as corrosion damage as shown in Figure 4.

3. Shear Buckling Failure Depending on the Corroded Stiffener Condition

3.1. FE Model Validation. To validate the FE analysis model used in this study, shear loading test results of a plate girder with similar dimension were compared, according to test boundary conditions and loading procedure [18]. Figure 5 shows validation model of the FE analysis. Figure 6 presents a comparison of the displacement at mid-span of the test

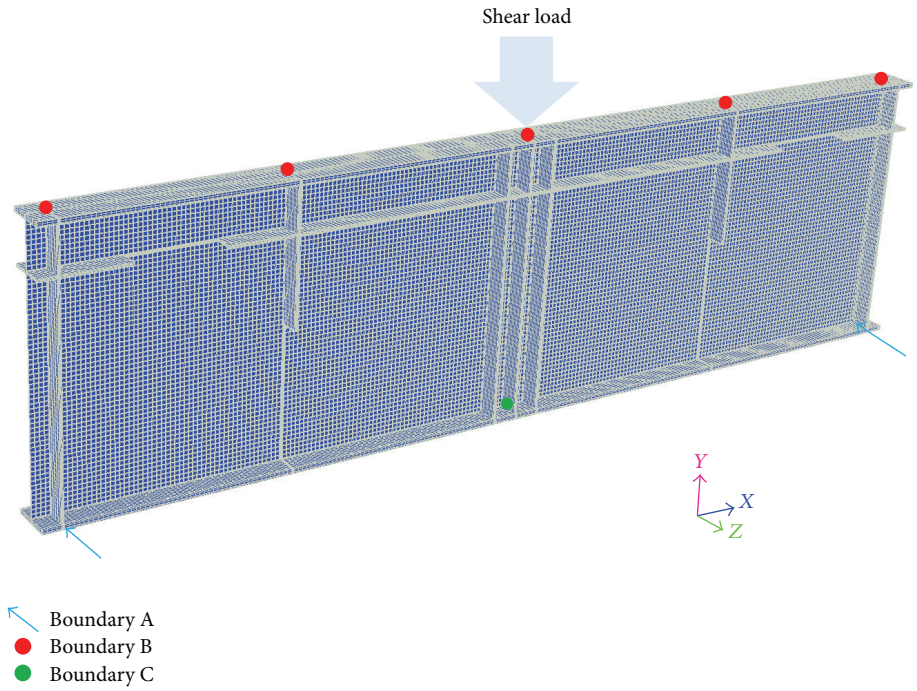

Figure 4: Boundary and load condition of the FE analysis model (V-LH600L400).

result data and the FE analysis result. As shown in Figure 6, its displacement was found to be in agreement with that of the test result. Therefore, the shear buckling behavior of the plate girder with stiffener can be examined using this FE analysis model.

3.2. Shear Buckling Failures of Web Panel with Corroded Stiffener. To examine the shear buckling failure mode of the web panel stiffened by vertical and longitudinal stiffeners depending on the corroded stiffener condition, shear buckling failure modes at shear bulking strength were compared. Figures 7–15 show their out-of-plane displacement contours and maximum principal stress contours. As shown in Figures 7–15, a typical shear buckling failure mode can be found with a diagonal tension field through the shear resistant behaviors of the web panel. By increasing the damage of the vertical stiffener, a wider and larger diagonal tension field band was present, owing to the increase caused in the shear resistant width of the web panel. Pronounced out-of-plane deformation also appeared at the corroded vertical stiffener, by reduction of the shear resistance of the vertical stiffener to restrict the shear buckling of the web panel; thus its tensile field shape was shown to be going down in the tension field direction of the web panel, according to decrease in the vertical stiffener by corrosion damage. For the 100% damage vertical stiffener, in particular, shear buckling failure mode of the wide web panel was present, due to increase in the width of the web panel by the disappearing vertical stiffener.

In the case of the vertical and left-longitudinal stiffeners corrosion model, as shown in Figures 10–13, their shear buckling failure modes were shown to be similar to those of the vertical stiffener corrosion model. A diagonal tension field was also present in the upper web panel of the longitudinal stiffener, according to increase in the corrosion damage of the longitudinal stiffener, except for the end-longitudinal stiffener case with 20% corrosion damage, and their tensile field shapes were shown to be more clearly going down in a tension field direction of the web panel affected by weak stiffened damaged stiffeners, according to decrease in the vertical stiffener by corrosion damage. The shear resistance of the end-longitudinal stiffener with 20% corrosion damage was not affected, and a similar diagonal tension field developed, even though corrosion damage occurred in the end-longitudinal stiffener. The vertical stiffener corrosion model with left-right longitudinal stiffener corrosion also showed a similar tendency to those of the vertical stiffener corrosion model with longitudinal stiffener corrosion, since the shear resistance of the web panel decreased by corrosion damage of the longitudinal stiffener of the next web panel, as shown in Figures 14–15.

To more clearly identify this tendency, out-of-plane displacements were also compared according to the corroded stiffener condition, in company with comparing the displacements at the center of a plate girder. Figure 16 shows the out-of-plane displacements and displacements of representative stiffener corrosion cases, as shown in Figures 7–15. Out-of-plane displacements at the center points of the end (left-) web panel appeared to increase, and their critical buckling loads and shear buckling strengths decreased with reduced stiffness effect of the stiffener for the shear resistant strength of the web plane, as shown in the load-displacement relationship curve in Figure 16. In their load out-of-plane displacement

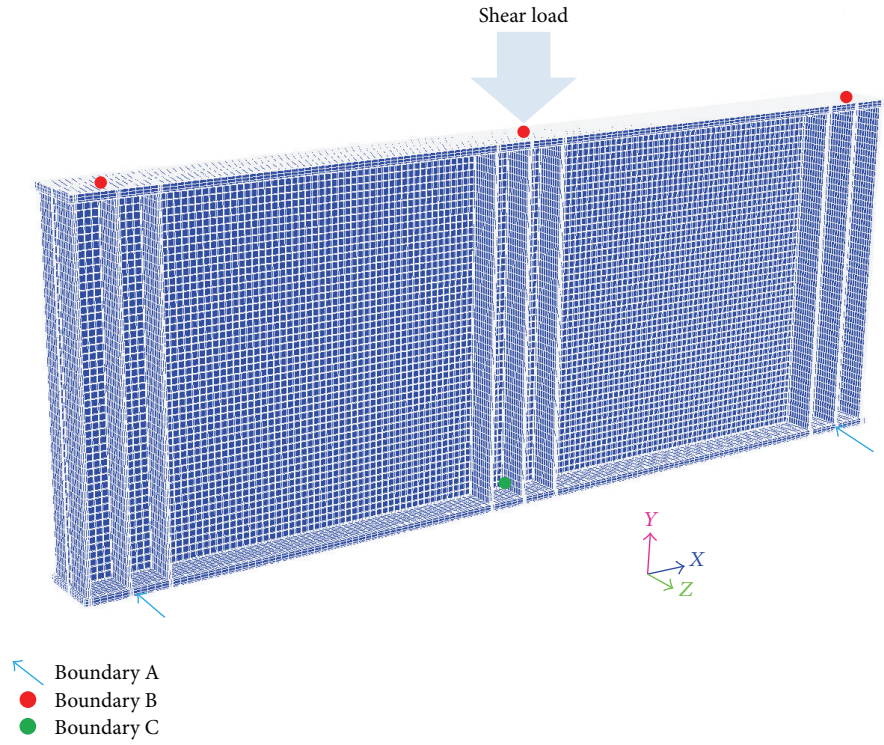

Figure 5: Validation model of the FE analysis.

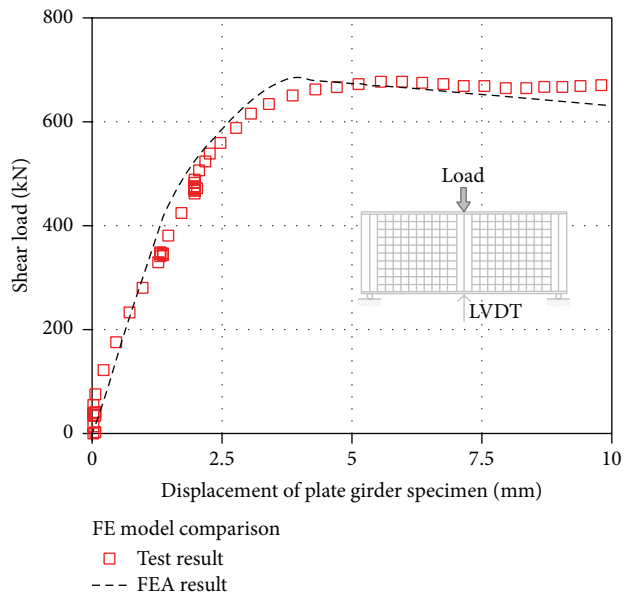

Figure 6: Comparison of the displacement at mid-span.

relationships, as shown in their shear buckling failure mode contours in Figures 7–15, distortional shear buckling behaviors of the web panel affected by the remaining vertical and longitudinal stiffeners presented as askew bends of the web plane to resist shear stress in the web panel. Since the point where the maximum out-of-plane displacement occurred changed, according to the mechanical relationship between the web panel and the vertical and longitudinal stiffeners in the plate girder, their load out-of-plane displacements at the center of the left web panel also showed different levels to the shear loading level, and irregular distribution in the same plane of the web panel.

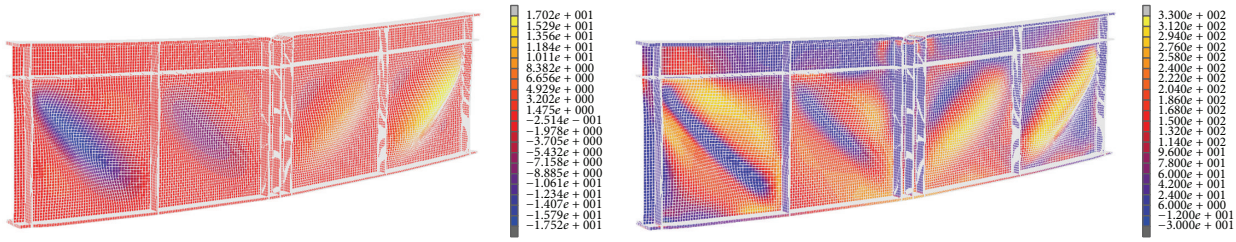

(a) Out-of-plane displacement contour (b) Maximum principal stress distribution contour

Figure 7: V-stiffener model with V: 0% corrosion damage (VH00).

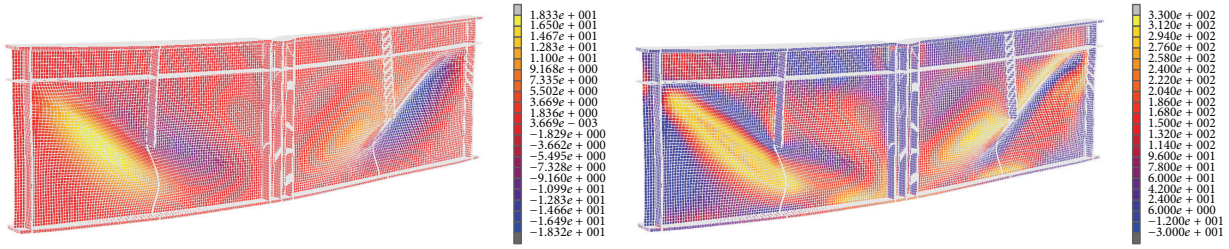

(a) Out-of-plane displacement contour (b) Maximum principal stress distribution contour

Figure 8: V-stiffener model with V: 50% corrosion damage (VH500).

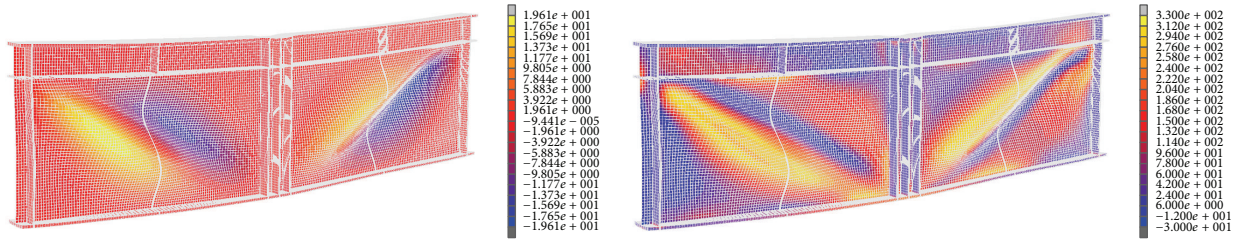

(a) Out-of-plane displacement contour (b) Maximum principal stress distribution contour

Figure 9: V-stiffener model with V: 100% corrosion damage (VH1000).

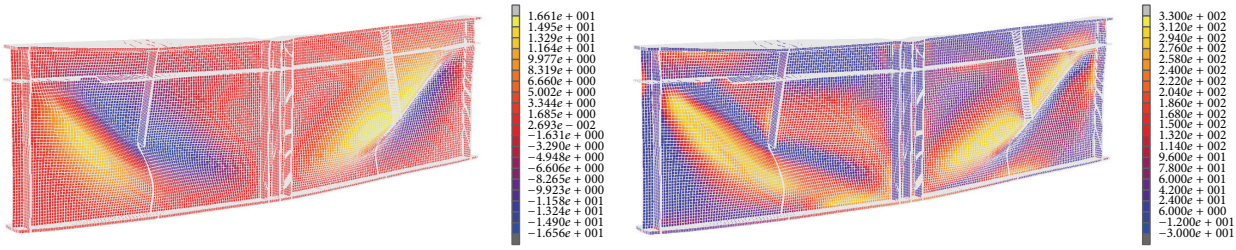

(a) Out-of-plane displacement contour (b) Maximum principal stress distribution contour

Figure 10: V-L stiffener model with V: 50% and L: 20% corrosion damage (V-LH500L200).

3.3. Shear Buckling Strength Related to Corroded Stiffener Condition

3.3.1. Vertical and Left-Longitudinal Stiffener Corrosion Model (V-L Cases). For the vertical and left-longitudinal stiffener corrosion model, the corrosion height of the vertical stiffener changed from 0 mm to 1000 mm in 100 mm units, and the corroded width of the end-longitudinal stiffener also changed from 0 mm to 1000 mm from the center of longitudinal stiffener in 200 mm units. Basically, their critical shear buckling load and shear buckling strength decreased, depending on the corroded stiffener height, as shown in Tables 1–6 and Figure 17. Their critical shear buckling load and shear buckling strength were also affected, according to the corroded width of the longitudinal stiffener. Thus, the critical shear buckling loads changed from 545.0 kN to 324.2 kN, and shear

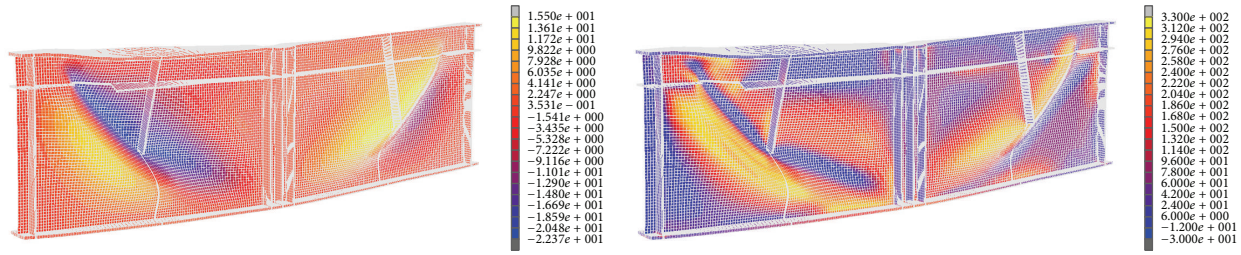

(a) Out-of-plane displacement contour (b) Maximum principal stress distribution contour

Figure 11: V-L stiffener model with V: 50% and L: 40% corrosion damage (V-LH500L400).

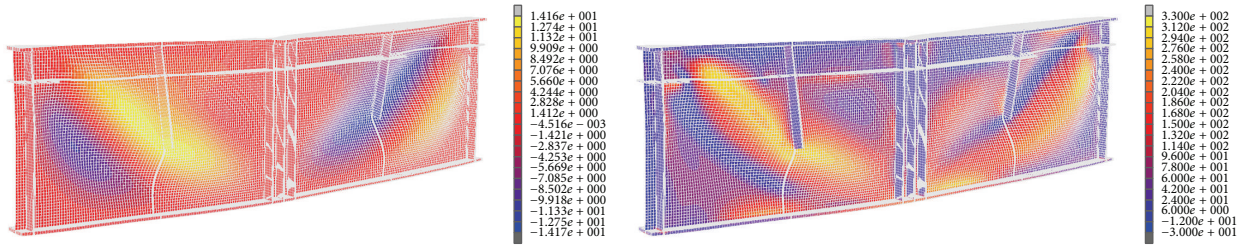

(a) Out-of-plane displacement contour (b) Maximum principal stress distribution contour

Figure 12: V-L stiffener model with V: 50% and L: 60% corrosion damage (V-LH500L600).

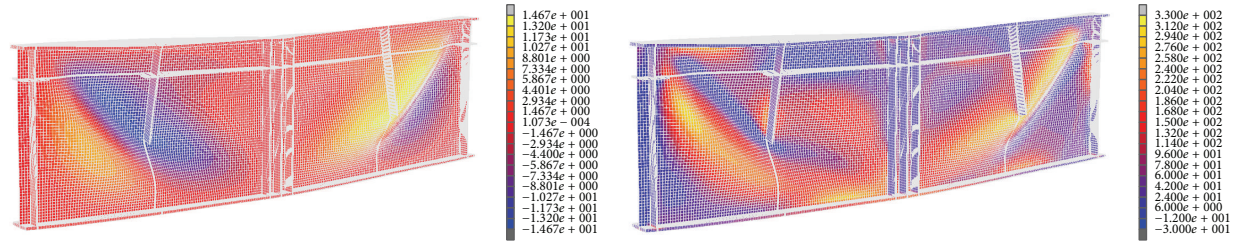

(a) Out-of-plane displacement contour (b) Maximum principal stress distribution contour

Figure 13: V-L stiffener model with V: 50% and L: 80% corrosion damage (V-LH500L800).

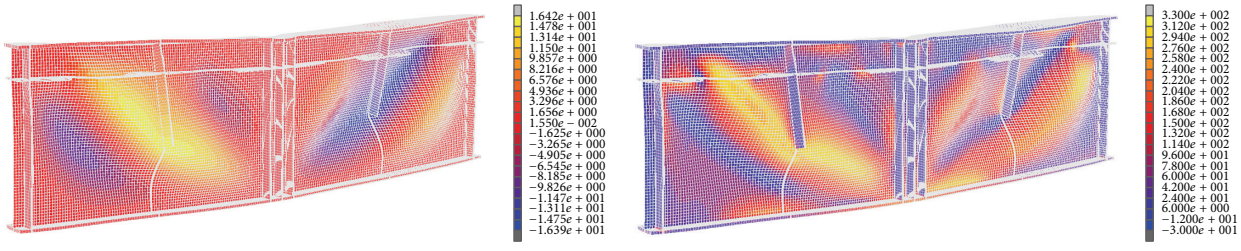

(a) Out-of-plane displacement contour (b) Maximum principal stress distribution contour

Figure 14: V-L-R stiffener model with V: 50%, L: 40%, and R: 40% corrosion damage (V-LH500L400R400).

buckling strengths decreased from 810.0 kN to 612.5 kN. This means the critical buckling load can decrease to 59% and 76% of those of the web panel stiffener without corrosion damage, according to the condition of the longitudinal stiffener. For each longitudinal stiffener corrosion case, their shear buckling values relatively sharply decreased, after 50% corrosion damage of the vertical stiffener, like that of the vertical stiffener corrosion model. Figure 18 summarizes the shear buckling ratio of each vertical and end-longitudinal stiffener corrosion model for no corrosion damage in the stiffener. For critical shear buckling load, it decreased from 82% to 59% of that of no corrosion damage in the stiffener. For shear buckling strength, it decreased from 88% to 76% of that of no corrosion damage in the stiffener.

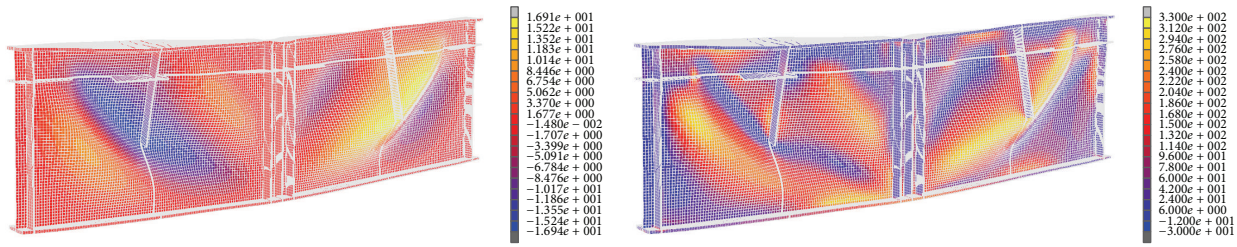

(a) Out-of-plane displacement contour

(b) Maximum principal stress distribution contour

Figure 15: V-L-R stiffener model with V: 50%, L: 40%, and R: 80% corrosion damage (V-LH500L400R800).

3.3.2. Vertical and Left-Right Longitudinal Stiffener Corrosion Model (V-L-R Cases). For the vertical and left-right longitudinal stiffener corrosion model, the corrosion height of the vertical stiffener changed from 0 mm to 500 mm in 100 mm units, and the corrosion width of the left-longitudinal stiffener changed from 200 mm to 800 mm in 200 mm units, and the right-longitudinal stiffener changed to 400 mm and 800 mm. As for the vertical and left-longitudinal stiffener corrosion model, they also show similar shear buckling behaviors with the change in the shear buckling value as shown in Tables 7–14 and Figure 19. As the shear stiffness of the enlarged shear web panel decreased from the disappearing longitudinal stiffener of the inner web panel (right web panel) by corrosion damage, their critical shear buckling loads and shear buckling strengths highly decreased by slightly more than those of the vertical and left- longitudinal stiffener corrosion model (V-L cases). For the same vertical stiffener corrosion, they thus have about 4~6% decreased shear buckling values affected by the next (near) longitudinal stiffener (longitudinal stiffener of the next panel). Figure 20 summarizes the shear buckling ratio of each vertical and left-right longitudinal stiffener corrosion model for no corrosion damage in the stiffener.

3.4. Evaluation of Shear Buckling Strength of Web Panel Related to Corroded Stiffener. Shear buckling behaviors of the web panel can be classified as before elastic shear buckling behavior, and post-shear buckling behavior, after elastic shear buckling behavior. Before elastic shear buckling, equal tensile and compressive principal stresses in the web panel develop prior to incipient buckling under shear load. After elastic shear buckling, the diagonal tension stresses (diagonal tension stresses) resist the additional shear load. Elastic shear buckling load is calculated by (1), using the buckling coefficient with regard to the boundary conditions [19]:

$$\tau_{cr} = k\frac{\pi^2 E}{12\left(1-\nu^2\right)}\left(\frac{t_w}{h_w}\right)^2 \quad \text{for } \frac{A_f}{A_w} < 0.8, \tag{1}$$

where E is the elastic modulus, ν is Poisson's ratio, t_w is the web thickness, h_w is the web height, and k is the buckling coefficient determined from the boundary conditions and the aspect ratio.

Shear buckling strength determined from post-shear buckling behaviors can be considered from AISC [20] and AASHTO [21] design specifications. In AISC [20], the nominal shear strength (V_n) is given by (2) and (3) at the limit of the tension field yielding. For the shear coefficient (C_v) of (3), it is suggested to be given by (4a), (4b), (4c):

$$V_n = 0.6 f_y A_w \quad \text{for } \frac{h_w}{t_w} \le 1.10\sqrt{\frac{k_v E}{f_y}}, \tag{2}$$

$$V_n = 0.6 f_y A_w \left(C_v + \frac{1-C_v}{1.15\sqrt{1+\left(d_0/h_w\right)^2}}\right) \quad \text{for } \frac{h_w}{t_w} > 1.10\sqrt{\frac{k_v E}{f_y}}, \tag{3}$$

$$C_v = 1.0 \quad \text{for } \frac{h_w}{t_w} \le 1.10\sqrt{\frac{k_v E}{f_y}}, \tag{4a}$$

$$C_v = 1.10\frac{\sqrt{k_v E/f_y}}{h_w/t_w} \quad \text{for } 1.10\sqrt{\frac{k_v E}{f_y}} < \frac{h_w}{t_w} \le 1.37\sqrt{\frac{k_v E}{f_y}}, \tag{4b}$$

$$C_v = \frac{1.51 k_v E}{\left(h_w/t_w\right)^2 f_y} \quad \text{for } 1.37\sqrt{\frac{k_v E}{f_y}} < \frac{h_w}{t_w}, \tag{4c}$$

where the buckling coefficient (k_v) is suggested to be given by

$$k_v = 5 + \frac{5}{\left(d_0/h_w\right)^2} = 5 \quad \text{when } \frac{d_0}{h_w} > 3 \text{ or } \frac{d_0}{h_w} > \left[\frac{260}{\left(h_w/t_w\right)^2}\right]. \tag{5}$$

In AASHTO [21], the nominal shear resistance (V_n) is given by (2), on the basis of the fully plastic strength (V_p), as shown in (6). The fully plastic shear strength (V_p) and the shear

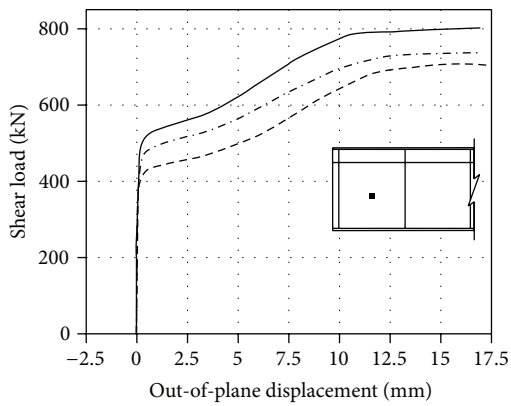

Out-of-plane displacement
- Corrosion damage: 0% V-stiffener and 0% L-stiffener
- Corrosion damage: 50% V-stiffener and 0% L-stiffener
- Corrosion damage: 100% V-stiffener and 0% L-stiffener

(a) Out-of-plane displacement of V-stiffener series

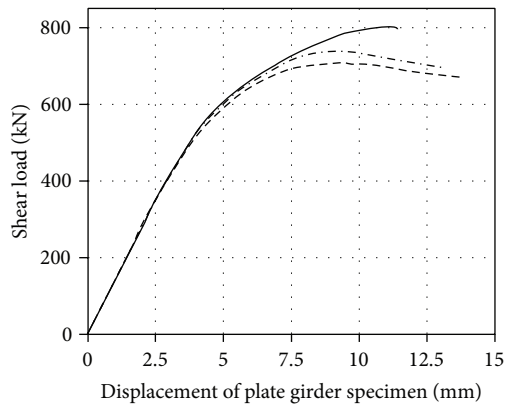

Displacement at center
- Corrosion damage: 0% V-stiffener and 0% L-stiffener
- Corrosion damage: 50% V-stiffener and 0% L-stiffener
- Corrosion damage: 100% V-stiffener and 0% L-stiffener

(b) Displacement of V-stiffener series

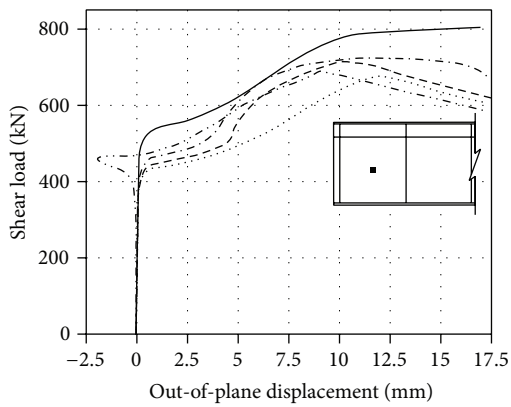

Out-of-plane displacement
- Corrosion damage: 0% V-stiffener and 0% L-stiffener
- Corrosion damage: 50% V-stiffener and 20% L-stiffener
- Corrosion damage: 50% V-stiffener and 40% L-stiffener
- Corrosion damage: 50% V-stiffener and 60% L-stiffener
- Corrosion damage: 50% V-stiffener and 80% L-stiffener

(c) Out-of-plane displacement of V-L stiffener series

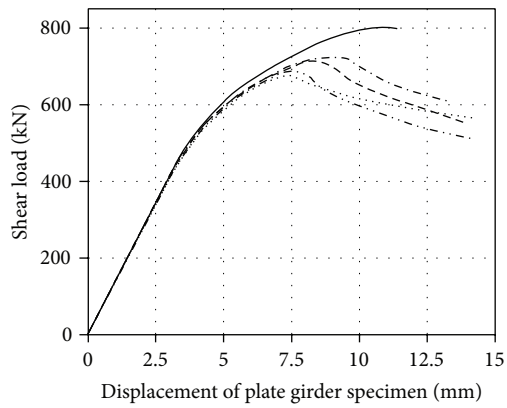

Displacement at center
- Corrosion damage: 0% V-stiffener and 0% L-stiffener
- Corrosion damage: 50% V-stiffener and 20% L-stiffener
- Corrosion damage: 50% V-stiffener and 40% L-stiffener
- Corrosion damage: 50% V-stiffener and 60% L-stiffener
- Corrosion damage: 50% V-stiffener and 80% L-stiffener

(d) Displacement of V-L stiffener series

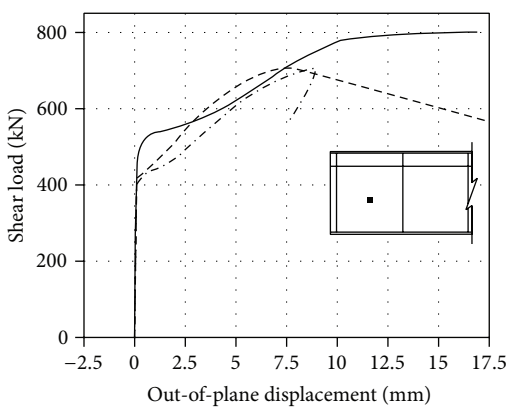

Out-of-plane displacement
- Corrosion damage: 0% V-stiffener and 0% L-stiffener
- Corrosion damage: 50% V-stiffener and 40-40% L&R-stiffener
- Corrosion damage: 50% V-stiffener and 40–80% L&R-stiffener

(e) Out-of-plane displacement of V-L-R-stiffener series

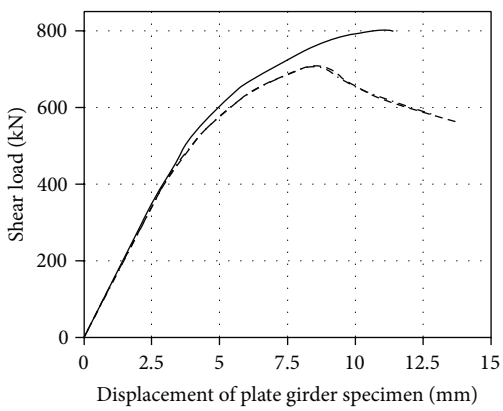

Displacement at center
- Corrosion damage: 0% V-stiffener and 0% L-stiffener
- Corrosion damage: 50% V-stiffener and 40-40% L&R-stiffener
- Corrosion damage: 50% V-stiffener and 40–80% L&R-stiffener

(f) Displacement of V-L-R-stiffener series

Figure 16: Displacement and out-of-plane displacement distribution of each case.

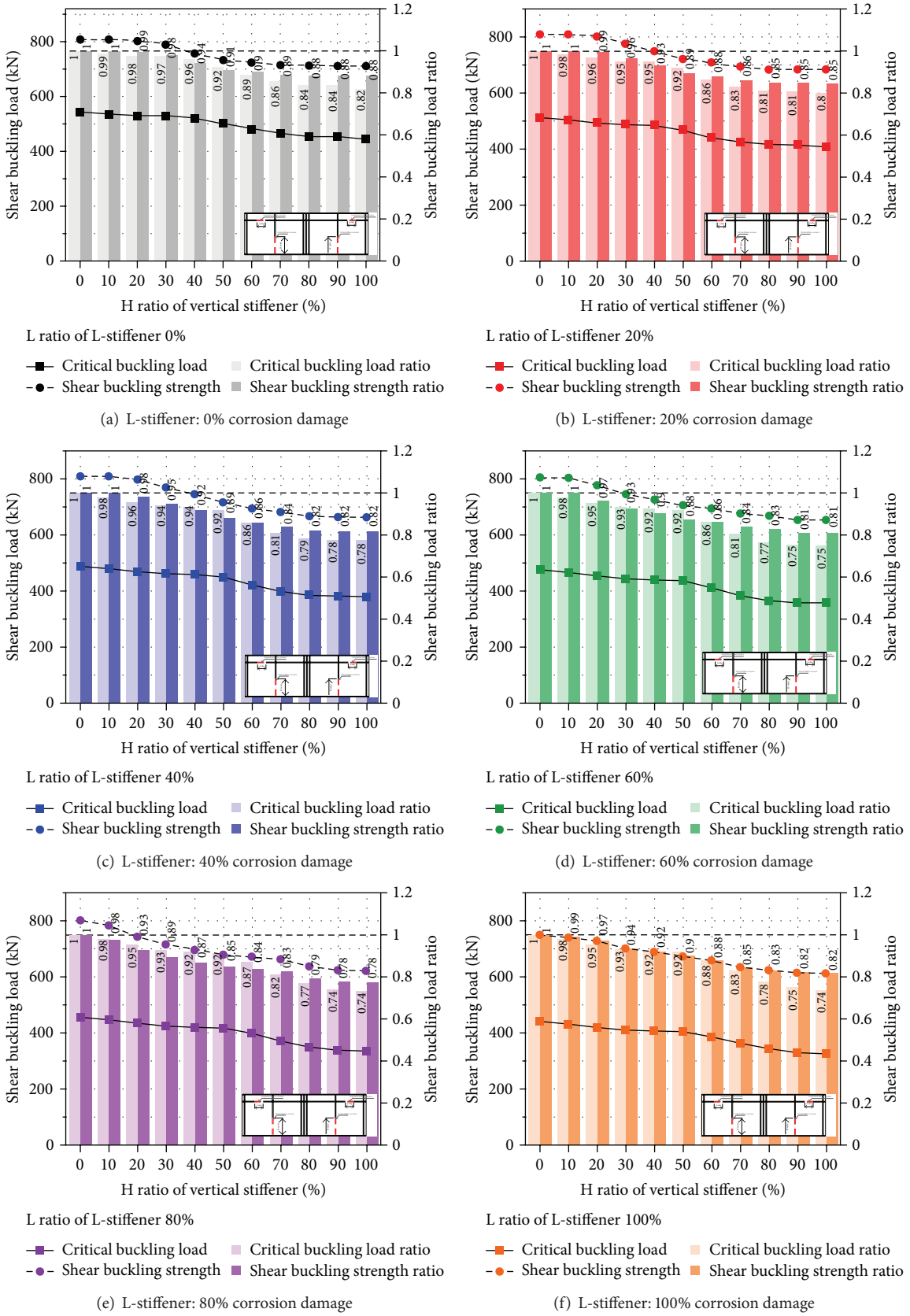

Figure 17: Shear buckling load and ratio of vertical and end-longitudinal stiffener corrosion model.

Table 1: Shear buckling values for V-LL00 stiffener series.

Corrosion of longitudinal stiffener	Corrosion of vertical stiffener		Critical shear buckling load (P_{cr})		Shear buckling strength (P_u)		With corrosion/without corrosion	
	Height (mm)	Ratio	Load (kN)	Ratio	Load (kN)	Ratio	P_{cr} ratio	P_u ratio
Width: 0 mm, ratio: 0%	0	0	545	1.00	810	1.00	1.00	1.00
	100	0.1	537.5	0.99	810	1.00	0.99	1.00
	200	0.2	532.5	0.98	805	0.99	0.98	0.99
	300	0.3	531	0.97	792.5	0.98	0.97	0.98
	400	0.4	523	0.96	760	0.94	0.96	0.94
	500	0.5	503.5	0.92	735	0.91	0.92	0.91
	600	0.6	482.8	0.89	727.5	0.90	0.89	0.90
	700	0.7	467.2	0.86	717.5	0.89	0.86	0.89
	800	0.8	458.05	0.84	715	0.88	0.84	0.88
	900	0.9	455.95	0.84	712.5	0.88	0.84	0.88
	1000	1.0	446.35	0.82	712.5	0.88	0.82	0.88

Table 2: Shear buckling values for V-LL200 stiffener series.

Corrosion of longitudinal stiffener	Corrosion of vertical stiffener		Critical shear buckling load (P_{cr})		Shear buckling strength (P_u)		With corrosion/without corrosion	
	Height (mm)	Ratio	Load (kN)	Ratio	Load (kN)	Ratio	P_{cr} ratio	P_u ratio
Width: 200 mm, ratio: 20%	0	0	513	1.00	810	1.00	0.94	1.00
	100	0.1	504	0.98	810	1.00	0.92	1.00
	200	0.2	494.35	0.96	802.5	0.99	0.91	0.99
	300	0.3	487.3	0.95	777.5	0.96	0.89	0.96
	400	0.4	485.35	0.95	750	0.93	0.89	0.93
	500	0.5	469.8	0.92	722.5	0.89	0.86	0.89
	600	0.6	443.6	0.86	710	0.88	0.81	0.88
	700	0.7	425.5	0.83	695	0.86	0.78	0.86
	800	0.8	416.95	0.81	685	0.85	0.77	0.85
	900	0.9	414.8	0.81	685	0.85	0.76	0.85
	1000	1.0	409.25	0.80	685	0.85	0.75	0.85

Table 3: Shear buckling values for V-LL400 stiffener series.

Corrosion of longitudinal stiffener	Corrosion of vertical stiffener		Critical shear buckling load (P_{cr})		Shear buckling strength (P_u)		With corrosion/without corrosion	
	Height (mm)	Ratio	Load (kN)	Ratio	Load (kN)	Ratio	P_{cr} ratio	P_u ratio
Width: 400 mm, ratio: 40%	0	0	489.15	1.00	810	1.00	0.90	1.00
	100	0.1	479.55	0.98	810	1.00	0.88	1.00
	200	0.2	469.15	0.96	797.5	0.98	0.86	0.98
	300	0.3	461.8	0.94	770	0.95	0.85	0.95
	400	0.4	459.85	0.94	745	0.92	0.84	0.92
	500	0.5	449.35	0.92	717.5	0.89	0.82	0.89
	600	0.6	420.8	0.86	695	0.86	0.77	0.86
	700	0.7	396.9	0.81	682.5	0.84	0.73	0.84
	800	0.8	385.1	0.79	667.5	0.82	0.71	0.82
	900	0.9	382.5	0.78	665	0.82	0.70	0.82
	1000	1.0	380.05	0.78	665	0.82	0.70	0.82

Table 4: Shear buckling values for V-LL600 stiffener series.

Corrosion of longitudinal stiffener	Corrosion of vertical stiffener		Critical shear buckling load (P_{cr})		Shear buckling strength (P_u)		With corrosion/without corrosion	
	Height (mm)	Ratio	Load (kN)	Ratio	Load (kN)	Ratio	P_{cr} ratio	P_u ratio
Width: 600 mm, ratio: 60%	0	0	475.15	1.00	805	1.00	0.87	0.99
	100	0.1	465.65	0.98	802.5	1.00	0.85	0.99
	200	0.2	453.25	0.96	777.5	0.97	0.83	0.96
	300	0.3	443.6	0.94	745	0.93	0.81	0.92
	400	0.4	438.9	0.94	725	0.90	0.81	0.90
	500	0.5	435.65	0.92	705	0.88	0.80	0.87
	600	0.6	409.85	0.86	692.5	0.86	0.75	0.85
	700	0.7	383.25	0.81	677.5	0.84	0.70	0.84
	800	0.8	364.05	0.79	667.5	0.83	0.67	0.82
	900	0.9	357.4	0.78	652.5	0.81	0.66	0.81
	1000	1.0	356.5	0.78	652.5	0.81	0.65	0.81

Table 5: Shear buckling values for V-LL800 stiffener series.

Corrosion of longitudinal stiffener	Corrosion of vertical stiffener		Critical shear buckling load (P_{cr})		Shear buckling strength (P_u)		With corrosion/without corrosion	
	Height (mm)	Ratio	Load (kN)	Ratio	Load (kN)	Ratio	P_{cr} ratio	P_u ratio
Width: 800 mm, ratio: 80%	0	0	455.5	1.00	802.5	1.00	0.84	0.99
	100	0.1	446.65	0.98	785	0.98	0.82	0.97
	200	0.2	434.3	0.95	745	0.93	0.80	0.92
	300	0.3	424	0.93	717.5	0.89	0.78	0.89
	400	0.4	419.25	0.92	697.5	0.87	0.77	0.86
	500	0.5	417.1	0.92	680	0.85	0.77	0.84
	600	0.6	397.45	0.87	672.5	0.84	0.73	0.83
	700	0.7	371.9	0.82	665	0.83	0.68	0.82
	800	0.8	350.45	0.77	637.5	0.79	0.64	0.79
	900	0.9	337.95	0.74	625	0.78	0.62	0.77
	1000	1.0	335	0.74	622.5	0.78	0.61	0.77

Table 6: Shear buckling values for V-LL1000 stiffener series.

Corrosion of longitudinal stiffener	Corrosion of vertical stiffener		Critical shear buckling load (P_{cr})		Shear buckling strength (P_u)		With corrosion/without corrosion	
	Height (mm)	Ratio	Load (kN)	Ratio	Load (kN)	Ratio	P_{cr} ratio	P_u ratio
Width: 100 mm, ratio: 100%	0	0	440.25	1.00	750	1.00	0.81	0.93
	100	0.1	431.65	0.98	742.5	0.99	0.79	0.92
	200	0.2	419.80	0.95	730	0.97	0.77	0.90
	300	0.3	410.10	0.93	702.5	0.94	0.75	0.87
	400	0.4	406.20	0.92	690	0.92	0.75	0.85
	500	0.5	404.00	0.92	675	0.90	0.74	0.83
	600	0.6	387.35	0.88	660	0.88	0.71	0.81
	700	0.7	363.7	0.83	635	0.85	0.67	0.78
	800	0.8	344.25	0.78	625	0.83	0.63	0.77
	900	0.9	330.85	0.75	617.5	0.82	0.61	0.76
	1000	1.0	324.20	0.74	612.5	0.82	0.59	0.76

Table 7: Shear buckling values for the V-L-RL200R400 stiffener series.

Corrosion of longitudinal stiffener		Corrosion of vertical stiffener		Critical shear buckling load (P_{cr})		Shear buckling strength (P_u)		With corrosion/without corrosion	
End (mm)	Inner (mm)	Height (mm)	Ratio	Load (kN)	Ratio	Load (kN)	Ratio	P_{cr} ratio	P_u ratio
200 (0.2)	400 (0.4)	0	0	515.5	1.00	770	1.00	0.95	0.95
		100	0.1	507.5	0.98	770	1.00	0.93	0.95
		200	0.2	498.7	0.97	770	1.00	0.92	0.95
		300	0.3	486.35	0.94	767.5	1.00	0.89	0.95
		400	0.4	472.55	0.92	747.5	0.97	0.87	0.92
		500	0.5	455.75	0.88	727.5	0.94	0.84	0.90

Table 8: Shear buckling values for the V-L-RL200R800 stiffener series.

Corrosion of longitudinal stiffener		Corrosion of vertical stiffener		Critical shear buckling load (P_{cr})		Shear buckling strength (P_u)		With corrosion/without corrosion	
End (mm)	Inner (mm)	Height (mm)	Ratio	Load (kN)	Ratio	Load (kN)	Ratio	P_{cr} ratio	P_u ratio
200 (0.2)	800 (0.8)	0	0	509	1.00	755	1.00	0.93	0.93
		100	0.1	507	1.00	755	1.00	0.93	0.93
		200	0.2	496.65	0.98	755	1.00	0.91	0.93
		300	0.3	476.1	0.94	752.5	1.00	0.87	0.93
		400	0.4	455.7	0.90	745	0.99	0.84	0.92
		500	0.5	438.75	0.86	720	0.95	0.81	0.89

Table 9: Shear buckling values for the V-L-RL400R400 stiffener series.

Corrosion of longitudinal stiffener		Corrosion of vertical stiffener		Critical shear buckling load (P_{cr})		Shear buckling strength (P_u)		With corrosion/without corrosion	
End (mm)	Inner (mm)	Height (mm)	Ratio	Load (kN)	Ratio	Load (kN)	Ratio	P_{cr} ratio	P_u ratio
400 (0.4)	400 (0.4)	0	0	488.4	1.00	770	1.00	0.90	0.95
		100	0.1	481.35	0.99	770	1.00	0.88	0.95
		200	0.2	472.8	0.97	770	1.00	0.87	0.95
		300	0.3	463.5	0.95	767.5	1.00	0.85	0.95
		400	0.4	454.7	0.93	742.5	0.96	0.83	0.92
		500	0.5	438.6	0.90	707.5	0.92	0.80	0.87

Table 10: Shear buckling values for the V-L-RL400R800 stiffener series.

Corrosion of longitudinal stiffener		Corrosion of vertical stiffener		Critical shear buckling load (P_{cr})		Shear buckling strength (P_u)		With corrosion/without corrosion	
End (mm)	Inner (mm)	Height (mm)	Ratio	Load (kN)	Ratio	Load (kN)	Ratio	P_{cr} ratio	P_u ratio
400 (0.4)	800 (0.8)	0	0	488.35	1.00	765	1.00	0.90	0.94
		100	0.1	482.4	0.99	762.5	1.00	0.89	0.94
		200	0.2	473.7	0.97	762.5	1.00	0.87	0.94
		300	0.3	459.95	0.94	762.5	1.00	0.84	0.94
		400	0.4	444.6	0.91	737.5	0.96	0.82	0.91
		500	0.5	428.6	0.88	707.5	0.92	0.79	0.87

Table 11: Shear buckling values for the V-L-RL600R400 stiffener series.

Corrosion of longitudinal stiffener		Corrosion of vertical stiffener		Critical shear buckling load (P_{cr})		Shear buckling strength (P_u)		With corrosion/without corrosion	
End (mm)	Inner (mm)	Height (mm)	Ratio	Load (kN)	Ratio	Load (kN)	Ratio	P_{cr} ratio	P_u ratio
600 (0.6)	400 (0.4)	0	0	475.45	1.00	770	1.00	0.87	0.95
		100	0.1	468	0.98	770	1.00	0.86	0.95
		200	0.2	457.35	0.96	770	1.00	0.84	0.95
		300	0.3	444.55	0.94	740	0.96	0.82	0.91
		400	0.4	432.8	0.91	702.5	0.91	0.79	0.87
		500	0.5	423.1	0.89	682.5	0.89	0.78	0.84

Table 12: Shear buckling values for the V-L-RL600R800 stiffener series.

Corrosion of longitudinal stiffener		Corrosion of vertical stiffener		Critical shear buckling load (P_{cr})		Shear buckling strength (P_u)		With corrosion/without corrosion	
End (mm)	Inner (mm)	Height (mm)	Ratio	Load (kN)	Ratio	Load (kN)	Ratio	P_{cr} ratio	P_u ratio
600 (0.6)	800 (0.8)	0	0	476.3	1.00	755	1.00	0.87	0.93
		100	0.1	469.3	0.99	755	1.00	0.86	0.93
		200	0.2	458.45	0.96	755	1.00	0.84	0.93
		300	0.3	442.25	0.93	742.5	0.98	0.81	0.92
		400	0.4	426.55	0.90	702.5	0.93	0.78	0.87
		500	0.5	414.35	0.87	680	0.90	0.76	0.84

Table 13: Shear buckling values for the V-L-RL800R400 stiffener series.

Corrosion of longitudinal stiffener		Corrosion of vertical stiffener		Critical shear buckling load (P_{cr})		Shear buckling strength (P_u)		With corrosion/without corrosion	
End (mm)	Inner (mm)	Height (mm)	Ratio	Load (kN)	Ratio	Load (kN)	Ratio	P_{cr} ratio	P_u ratio
800 (0.8)	400 (0.4)	0	0	458.45	1.00	772.5	1.00	0.84	0.95
		100	0.1	450.45	0.98	772.5	1.00	0.83	0.95
		200	0.2	438.3	0.96	745	0.96	0.80	0.92
		300	0.3	424.45	0.93	707.5	0.92	0.78	0.87
		400	0.4	413.8	0.90	682.5	0.88	0.76	0.84
		500	0.5	407.8	0.89	667.5	0.86	0.75	0.82

Table 14: Shear buckling values for the V-L-RL800R800 stiffener series.

Corrosion of longitudinal stiffener		Corrosion of vertical stiffener		Critical shear buckling load (P_{cr})		Shear buckling strength (P_u)		With corrosion/without corrosion	
End (mm)	Inner (mm)	Height (mm)	Ratio	Load (kN)	Ratio	Load (kN)	Ratio	P_{cr} ratio	P_u ratio
800 (0.8)	800 (0.8)	0	0	460.8	1.00	755	1.00	0.85	0.93
		100	0.1	451.85	0.98	755	1.00	0.83	0.93
		200	0.2	439	0.95	742.5	0.98	0.81	0.92
		300	0.3	422.6	0.92	707.5	0.94	0.78	0.87
		400	0.4	409.55	0.89	682.5	0.90	0.75	0.84
		500	0.5	401.4	0.87	665	0.88	0.74	0.82

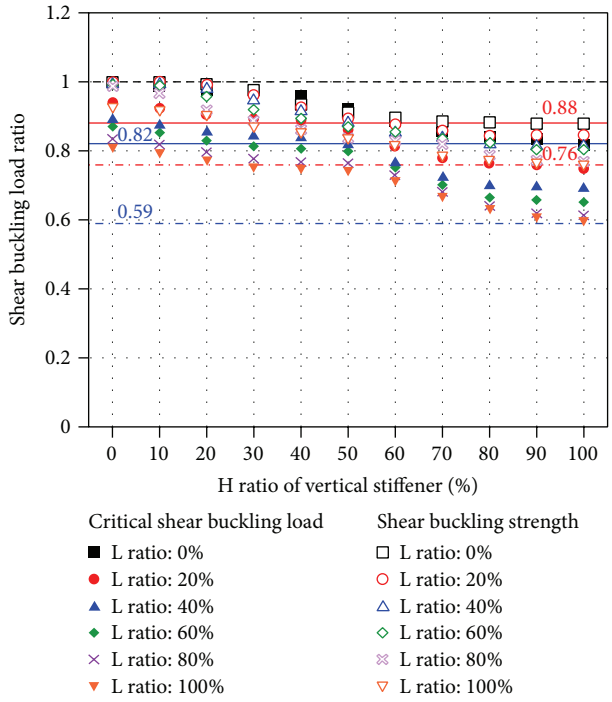

Figure 18: Shear buckling ratio of V-L stiffener corrosion series for no corrosion damage.

coefficient (C_v) of (6) are suggested to be given by (7) and (8a), (8b), and (8c), respectively:

$$V_n = V_p\left(C_v + \frac{0.87\,(1 - C_v)}{\sqrt{1 + (d_0/h_w)^2}}\right), \tag{6}$$

$$V_p = \tau_y h_w t_w = \frac{f_y}{\sqrt{3}} h_w t_w = 0.58 f_y h_w t_w, \tag{7}$$

$$C_v = 1.0 \quad \text{for } \frac{h_w}{t_w} \le 1.12\sqrt{\frac{k_v E}{f_y}}, \tag{8a}$$

$$C_v = 1.12\frac{\sqrt{k_v E/f_y}}{h_w/t_w}, \quad \text{for } 1.12\sqrt{\frac{k_v E}{f_y}} < \frac{h_w}{t_w} \le 1.40\sqrt{\frac{k_v E}{f_y}}, \tag{8b}$$

$$C_v = \frac{1.57 k_v E}{(h_w/t_w)^2 f_y}, \quad \text{for } 1.40\sqrt{\frac{k_v E}{f_y}} < \frac{h_w}{t_w}, \tag{8c}$$

where the buckling coefficient (k_v) is suggested to be as shown in

$$k_v = 5 + \frac{5}{(d_0/h_w)^2}. \tag{9}$$

For calculation by AASHTO and AISC design specifications, the critical shear buckling load of web panel (1000 × 1000 mm) using (4a), (4b), and (4c) was calculated as 402 kN, and the shear buckling strength of the web panel was calculated as 709 kN for AASHTO, and 731 kN for AISC. In this study, vertical stiffener cases with 0~100% corrosion damage have been considered to examine the effect of corrosion damage of the stiffener on shear buckling behaviors of the web panel. However, it is difficult for a vertical stiffener to fully corrode (100% corrosion) under a real atmospheric corrosion environment. Therefore, the shear buckling strength of vertical stiffener cases with 0~50% corrosion damage was considered, to compare the shear buckling values of the web panel stiffened by stiffeners with design values. Figure 21 shows a comparison of the shear buckling strengths for each analysis case of the stiffener corrosion model. As shown in Figure 21, on the whole, shear buckling strengths of the web panels stiffened by stiffeners were shown to be higher than the design value, except for the multiply severely corroded stiffener cases. However, after 40% corrosion damage of the vertical stiffener, its shear buckling strength can decrease below the design value. Therefore, the corrosion ratio of the vertical stiffener should be checked, to repair or reinforce the web panel with a corroded stiffener.

4. Conclusions

This study examined the shear buckling failure and strength of web panels stiffened by stiffeners, to evaluate the effect of corroded stiffeners on shear buckling behaviors, according to the local corrosion damage of the stiffener. Therefore, for stiffener corrosion cases in the plate girder, nonlinear FE analyses were conducted, and their shear buckling behaviors

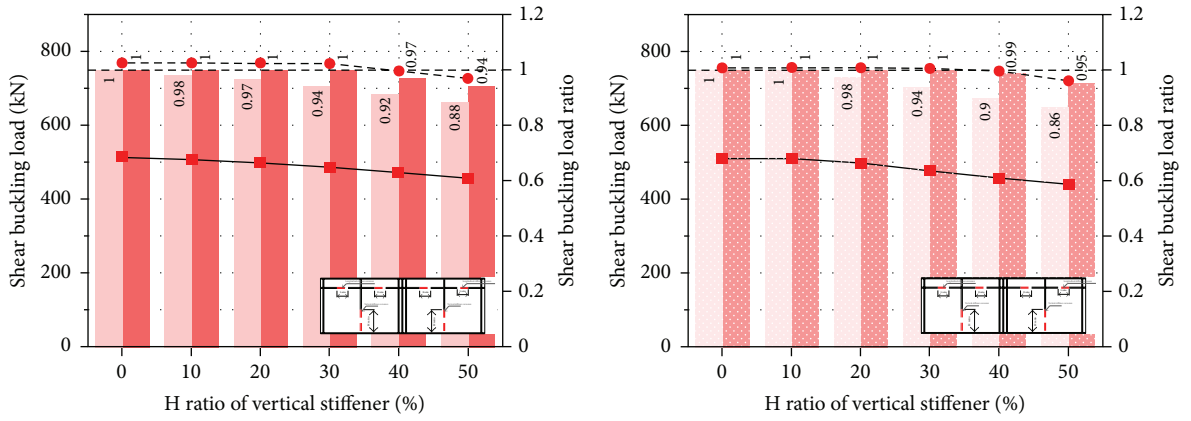

(a) L-stiffener: 20–40% corrosion damage

(b) L-stiffener: 20–80% corrosion damage

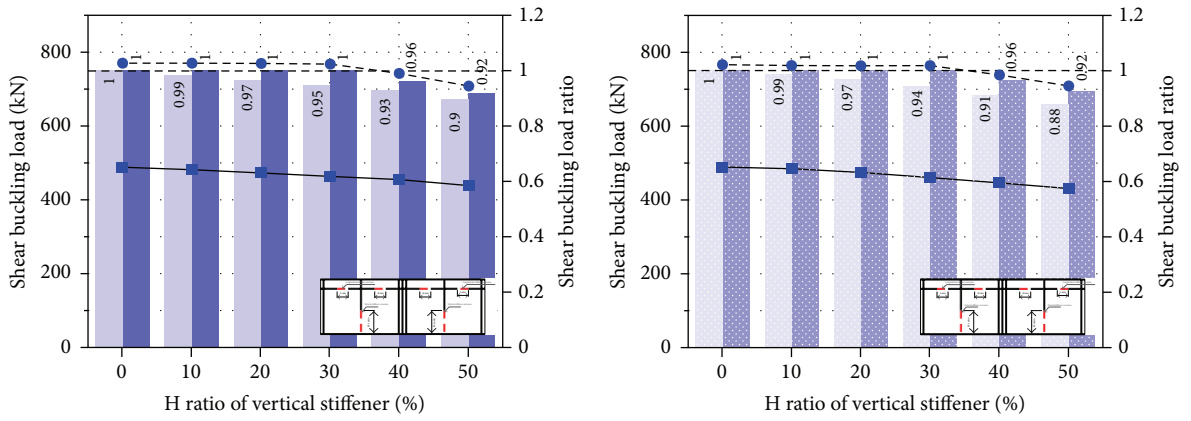

(c) L-stiffener: 40-40% corrosion damage

(d) L-stiffener: 40–80% corrosion damage

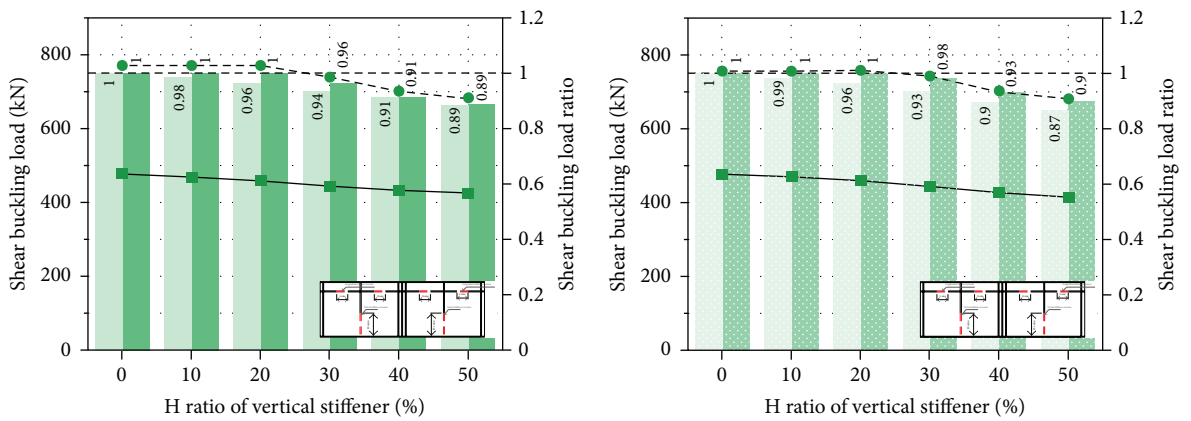

(e) L-stiffener: 60–40% corrosion damage

(f) L-stiffener: 60–80% corrosion damage

Figure 19: Continued.

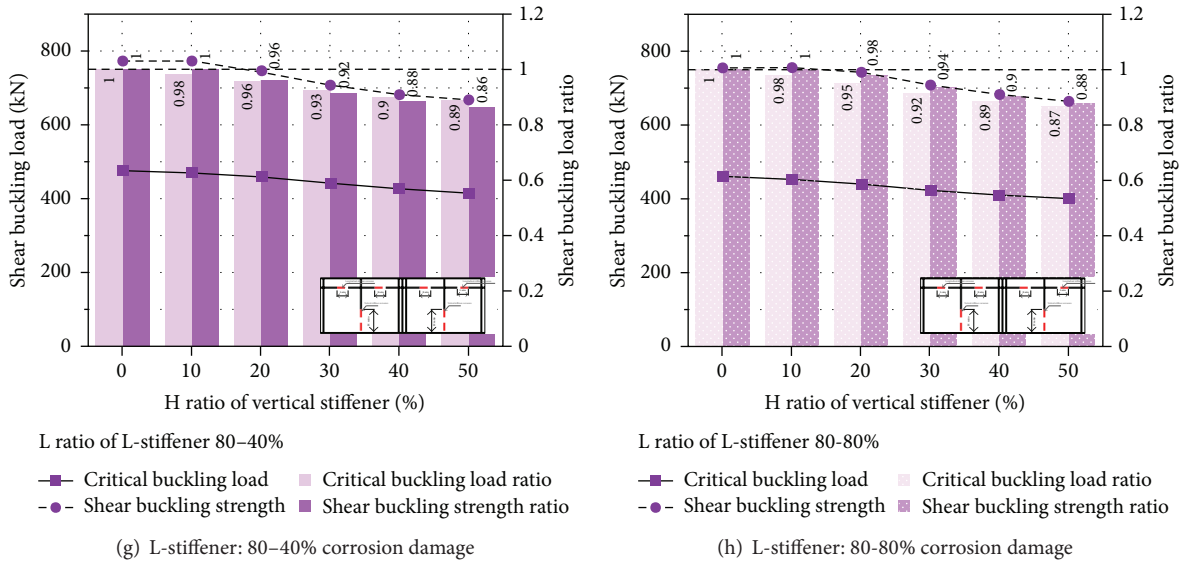

(g) L-stiffener: 80–40% corrosion damage (h) L-stiffener: 80-80% corrosion damage

Figure 19: Shear buckling load and ratio of the V-L-R stiffener corrosion model.

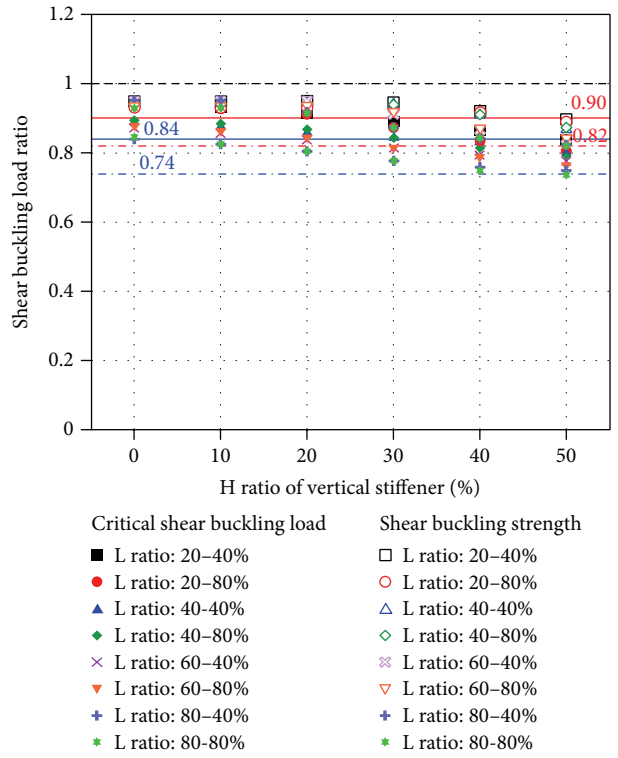

Figure 20: Shear buckling ratio of V-L-R stiffener corrosion series for no corrosion damage.

were compared, as well as the change in the shear buckling strength of the web panel, depending on the degree of corrosion of the vertical and longitudinal stiffeners. For shear buckling failure mode, basically, they were shown to have a typical shear buckling failure mode, related to the shear resistance of a web panel with a diagonal tension field. Their tensile field band shapes were more clearly going down in a tension field direction of the web panel affected by weak stiffened damaged stiffeners, depending on the degree of corrosion damage of the vertical stiffener. This tendency can be found in the load out-of-plane displacement in the center web panel, and the maximum out-of-plane displacement also changed, according to the mechanical relationship between the web panel and the vertical and longitudinal stiffeners in the plate girder. Their critical shear buckling load and shear buckling strength decreased, depending on the corroded

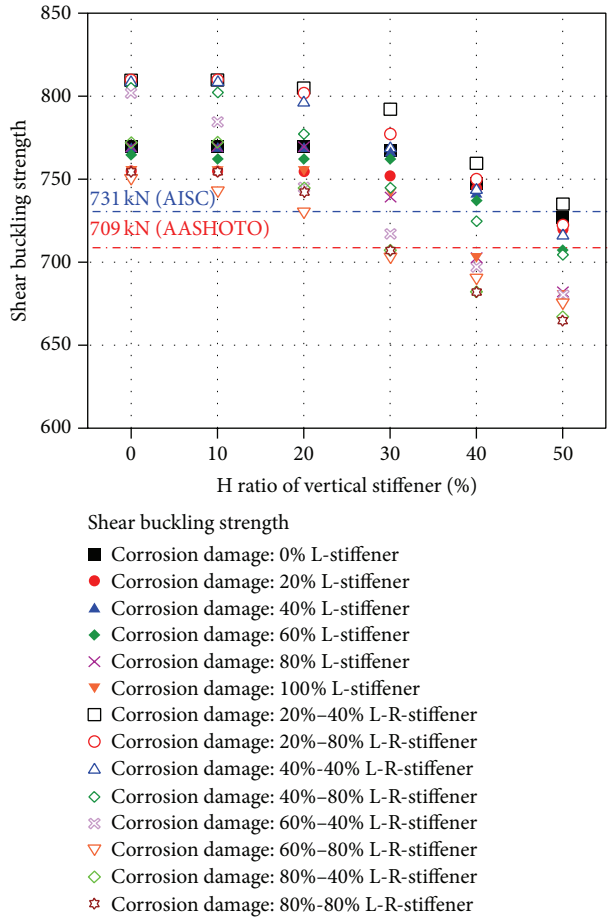

Figure 21: Comparison of the shear buckling strengths for each analysis case.

height of the vertical stiffener and the corroded width of the longitudinal stiffener from 82% to 59% of the critical shear buckling load, and from 88% to 76% of the shear buckling strength, since the shear buckling behaviors of the web panel are determined by the shear resistance of the web panel stiffened by each stiffener. For over 40% corrosion damage of the vertical stiffener, the corrosion ratio of the vertical stiffener should be considered to repair or reinforce the web panel with a corroded stiffener, since their shear buckling strengths can decrease below the design value.

In this study, the shear buckling behaviors of a web panel stiffened by stiffener with corrosion damage were examined. Their shear buckling failure behaviors and the change in the shear buckling strength were found to be insufficient for all web panel conditions with stiffener. For more effective results on the shear buckling behavior of web panel, various design conditions of the web panel and the corrosion conditions should be considered.

Conflict of Interests

The authors declare that there is no conflict of interests regarding the publication of this paper.

Acknowledgment

This research was supported by Basic Science Research Program through the National Research Foundation of Korea (NRF) funded by the Ministry of Education (NRF-2014R1A1A2055900 and NRF-2014R1A1A2058765).

References

[1] National Institute for Land and Infrastructure Management, "Research on local corrosion of highway steel bridges," Technical Note 294, National Institute for Land and Infrastructure Management, 2006 (Japanese).

[2] I.-T. Kim, M.-J. Lee, J.-H. Ahn, and S. Kainuma, "Experimental evaluation of shear buckling behaviors and strength of locally corroded web," *Journal of Constructional Steel Research*, vol. 83, pp. 75–89, 2013.

[3] J.-H. Ahn, I.-T. Kim, S. Kainuma, and M.-J. Lee, "Residual shear strength of steel plate girder due to web local corrosion," *Journal of Constructional Steel Research*, vol. 89, pp. 198–212, 2013.

[4] T. Shimozato, Y. Tamaki, J. Murakoshi, and M. Takahasi, "Real time monitoring of bridge collapse due to intense corrosion," *Magazine of Korean Society of Steel Construction*, vol. 22, no. 5, pp. 13–17, 2010 (Korean).

[5] D. M. Porter, K. C. Rockey, and H. R. Evans, "The collapse behavior of plate girders loaded in shear," *Structural Engineer*, vol. 53, no. 8, pp. 313–325, 1975.

[6] S. C. Lee, J. S. Davidson, and C. H. Yoo, "Shear buckling coefficients of plate girder web panels," *Computers & Structures*, vol. 59, no. 5, pp. 789–795, 1996.

[7] S.-K. Jung and D. W. White, "Shear strength of horizontally curved steel I-girders—finite element analysis studies," *Journal of Constructional Steel Research*, vol. 62, no. 4, pp. 329–342, 2006.

[8] I. Estrada, E. Real, and E. Mirambell, "Shear resistance in stainless steel plate girders with transverse and longitudinal stiffening," *Journal of Constructional Steel Research*, vol. 64, no. 11, pp. 1239–1254, 2008.

[9] N. C. Hagen and P. K. Larsen, "Shear capacity of steel plate girders with large web openings—part II: design guidelines," *Journal of Constructional Steel Research*, vol. 65, no. 1, pp. 151–158, 2009.

[10] M. F. Hassanein, "Finite element investigation of shear failure of lean duplex stainless steel plate girders," *Thin-Walled Structures*, vol. 49, no. 8, pp. 964–973, 2011.

[11] M. M. Alinia, A. Gheitasi, and M. Shakiba, "Postbuckling and ultimate state of stresses in steel plate girders," *Thin-Walled Structures*, vol. 49, no. 4, pp. 455–464, 2011.

[12] A. Bedynek, E. Real, and E. Mirambell, "Tapered plate girders under shear: tests and numerical research," *Engineering Structures*, vol. 46, pp. 350–358, 2013.

[13] J.-H. Ahn, S. Kainuma, and I.-T. Kim, "Shear failure behaviors of a web panel with local corrosion depending on web boundary conditions," *Thin-Walled Structures*, vol. 73, pp. 302–317, 2013.

[14] T. E. Dunbar, N. Pegg, F. Taheri, and L. Jiang, "A computational investigation of the effects of localized corrosion on plates and stiffened panels," *Marine Structures*, vol. 17, no. 5, pp. 385–402, 2004.

[15] D. Ok, Y. Pu, and A. Incecik, "Computation of ultimate strength of locally corroded unstiffened plates under uniaxial compression," *Marine Structures*, vol. 20, no. 1-2, pp. 100–114, 2007.

[16] R. Rahgozar, "Remaining capacity assessment of corrosion damaged beams using minimum curves," *Journal of Constructional Steel Research*, vol. 65, no. 2, pp. 299–307, 2009.

[17] J. E. Silva, Y. Garbatov, and C. Guedes Soares, "Ultimate strength assessment of rectangular steel plates subjected to a random localised corrosion degradation," *Engineering Structures*, vol. 52, pp. 295–305, 2013.

[18] J.-H. Ahn, W.-H. Lee, and I.-T. Kim, "Shear buckling of the web panel in the plate girder with circular local section damage," in *Proceedings of the 25th Annual Conference Korean Society of Steel Construction*, vol. 25, pp. 91–92, 2014 (Korean).

[19] S. P. Timoshenko and J. M. Gere, *Theory of Elastic Stability*, McGraw-Hill, New York, NY, USA, 2nd edition, 1961.

[20] American Institute of Steel Construction, *Seismic Provisions for Structural Steel Buildings*, AISC, Chicago, Ill, USA, 2005.

[21] American Association of State Highway and Transportation Officials, *LRFD Bridge Design Specifications*, AASHTO, Washington, DC, USA, 1st edition, 1994.